

Metalloenzymes

Deutsche Ausgabe: DOI: 10.1002/ange.201511896
Internationale Ausgabe: DOI: 10.1002/anie.201511896**[FeFe]-Hydrogenase with Chalcogenide Substitutions at the H-Cluster Maintains Full H₂ Evolution Activity**Jens Noth, Julian Esselborn, Jörn Güldenhaupt, Annika Brünje, Anne Sawyer, Ulf-Peter Apfel,*
Klaus Gerwert, Eckhard Hofmann, Martin Winkler, and Thomas Happe*

Abstract: The [FeFe]-hydrogenase HYDA1 from *Chlamydomonas reinhardtii* is particularly amenable to biochemical and biophysical characterization because the H-cluster in the active site is the only inorganic cofactor present. Herein, we present the complete chemical incorporation of the H-cluster into the HYDA1-apoprotein scaffold and, furthermore, the successful replacement of sulfur in the native [4Fe_H] cluster with selenium. The crystal structure of the reconstituted pre-mature HYDA1-[4Fe4Se]_H protein was determined, and a catalytically intact artificial H-cluster variant was generated upon in vitro maturation. Full hydrogen evolution activity as well as native-like composition and behavior of the redesigned enzyme were verified through kinetic assays, FTIR spectroscopy, and X-ray structure analysis. These findings reveal that even a bioinorganic active site with exceptional complexity can exhibit a surprising level of compositional plasticity.

With turnover frequencies of up to 10⁴ molecules of dihydrogen (H₂) per second, [FeFe]-hydrogenases are the fastest known biocatalysts for the reduction of protons to H₂.^[1] There are several types of [FeFe]-hydrogenases, which differ not only in protein structure and composition, but also in the number of accessory [FeS]-clusters, which act as an electron (e⁻) relay between the e⁻-mediator docking site and the active center (H-cluster) of the enzyme.^[2] The H-cluster is a complex inorganic cofactor, consisting of a cysteine-coordinated [4Fe4S]-cluster ([4Fe_H]) linked to a unique [2Fe2S]-subcluster ([2Fe_H]) with three CO and two CN⁻ ligands. An azadithiolate (adt = -S-CH₂-NH-CH₂-S-) ligand, bridging both Fe sites in [2Fe_H] (proximal (Fe_p) and distal (Fe_d) relative to the [4Fe_H]-moiety) is essential for fast proton shuttling to and from the vacant ligand site at Fe_d,^[3] where proton reduction and H₂ oxidation occur (Figure 1A).^[1c,4] Owing to its structural simplicity, the monomeric hydrogenase, HYDA1, from the unicellular green alga *Chlamydomonas reinhardtii*, is a model enzyme for studying the catalytic features of [FeFe]-hydrogenases. As the H-cluster is the only bioinorganic

cofactor in the algal enzyme, spectroscopy can be used to directly probe its metal cofactor. Furthermore, HYDA1 can be efficiently expressed and purified with high yields in *Escherichia coli*.^[5] While standard [FeS]-clusters, including the [4Fe_H]-moiety of the H-cluster, can be synthesized in vivo by housekeeping iron-sulfur cluster biosynthetic machineries,^[6] the formation of the unique [2Fe_H]-subsite depends on the three highly specific maturation factors, HYDE, -F, and -G.^[7] Recently, we found that the complex maturation pathway, which does not natively occur in *E. coli*, can be bypassed in vitro by adding the synthetic [2Fe_H]-analogue [Fe₂(CO)₄(CN)₂(adt)]²⁻ ([2Fe_H]^{MIM}) to the inactive pre-mature HYDA1[4Fe_H], rapidly yielding a fully functional enzyme.^[3a,b]

In the present study, we applied this tool of in vitro maturation, in combination with the technique of chemical [FeS]-cluster reconstitution,^[8] to demonstrate that H-cluster manipulation is not confined to the [2Fe_H]-site,^[3a,b] but can be extended to the [4Fe_H]-moiety, thus enabling the artificial synthesis and manipulation of the complete H-cluster architecture.

The [2Fe_H]- and the [4Fe_H]-cluster play synergistic roles in the catalytic cycle of the H-cluster. Both subsites are coupled by only one bridging cysteine ligand, resulting in a functional unit through which electrons are reversibly shuttled between the location of substrate turnover at Fe_d and external e⁻-mediators that dock at the entrance of the e⁻-relay ([4Fe_H]) (Figure 1A).^[9] In 2009, chemical reconstitution was shown for the first time for the biosynthesized *C. reinhardtii* HYDA1 [4Fe_H] cubane cluster, further denoted as [4Fe4S]_H.^[10] Two concurrent studies revealed that a pre-formed cubane cluster is essential for HYDF-mediated incorporation of the [2Fe_H]-subsite into HYDA1. As the tertiary protein structure folds around the cubane cluster, the essential framework is prepared for the functional incorporation of the substrate-binding [2Fe_H]-cluster. The redox features and protonation state of the [2Fe_H]-subcluster change while passing through the catalytic steps of the turnover cycle. Three main catalytic

[*] Dr. J. Noth, Dr. J. Esselborn, A. Brünje, Dr. A. Sawyer, Dr. M. Winkler, Prof. T. Happe
Ruhr Universität Bochum
Lehrstuhl für Biochemie der Pflanzen, AG Photobiotechnologie
Universitätsstrasse 150, 44801 Bochum (Germany)
E-mail: thomas.happe@ruhr-uni-bochum.de
Dr. J. Güldenhaupt, Prof. K. Gerwert
Ruhr Universität Bochum
Lehrstuhl für Biophysik, AG Spektroskopie
Universitätsstrasse 150, 44801 Bochum (Germany)

Prof. E. Hofmann
Ruhr Universität Bochum
Lehrstuhl für Biophysik, AG Röntgenstrukturanalyse an Proteinen
Universitätsstrasse 150, 44801 Bochum (Germany)
Dr. U.-P. Apfel
Ruhr Universität Bochum
Fakultät für Chemie und Biochemie
Lehrstuhl für Anorganische Chemie I/ Bioanorganische Chemie
Universitätsstrasse 150, 44801 Bochum (Germany)
E-mail: ulf.apfel@ruhr-uni-bochum.de

Supporting information for this article can be found under:
<http://dx.doi.org/10.1002/anie.201511896>.

states are clearly distinguishable by infrared spectroscopy. The crucial participation of the $[4\text{Fe}_\text{H}]$ -site in the catalytic cycle became obvious after the discovery that the two-fold reduced H_{red} state is part of the reaction mechanism, which unlike H_{ox} and H_{red} , exhibits a reduced $[4\text{Fe}_\text{H}]$ -site.^[4,11] Therefore, in contrast to other reported examples of chalcogenide replacement in $[\text{FeS}]$ -clusters, such as those of plant type and bacterial ferredoxins,^[12] the $[4\text{Fe}_\text{H}]$ -cluster targeted here is an essential part of the catalytic cofactor itself.

Cluster-free HYDA1 $[\Delta\text{H}]$ was prepared by removing the in-vivo-incorporated $[4\text{Fe}_\text{H}]$ -cluster from native HYDA1- $[4\text{Fe}_\text{H}]$. This HYDA1 $[\Delta\text{H}]$, as shown previously,^[10] did not display catalytic H_2 -production activity upon addition of $[2\text{Fe}_\text{H}]^{\text{MIM}}$ (Figure 1B). This allowed us to monitor time-resolved $[4\text{Fe}_\text{H}]$ -cluster reconstitution by measuring enzyme activity after in vitro activation with synthesized $[2\text{Fe}_\text{H}]^{\text{MIM}}$ (Figure 1B).

HYDA1 $[\Delta\text{H}]$ reconstitution mixtures in which only Fe^{2+} or one of the chalcogenides (S^{2-} or Se^{2-}) were added did not reveal any significant H_2 evolution activity ($< 3\%$ compared to $\text{Fe}^{2+}/\text{S}^{2-}$ -reconstituted HYDA1 (HYDA1 $[4\text{Fe}4\text{S}]_\text{H}$)) upon addition of $[2\text{Fe}_\text{H}]^{\text{MIM}}$, indicating the successful removal of the bio-assembled $[4\text{Fe}_\text{H}]$ during preparation of HYDA1 $[\Delta\text{H}]$ (Figure 1B). Notably, reconstitution mixtures containing HYDA1 $[\Delta\text{H}]$, in combination with Fe^{2+} and either S^{2-} or Se^{2-} , exhibited strongly increasing H_2 production activities over time upon in vitro maturation, with maximum rates occurring after 19 h (Figure 1B). In comparison to the $\text{Fe}^{2+}/\text{S}^{2-}$ samples, the reconstitution kinetics for cluster assembly of the $\text{Fe}^{2+}/\text{Se}^{2-}$ combination were slightly slower in the first hours. However, the maximum specific activity after in vitro maturation did not deviate significantly from that observed after reconstitution with Fe^{2+} and S^{2-} (Figure 1B,C). Upon reconstitution with Fe^{2+} and either S^{2-} or Se^{2-} , activities of almost $600 \mu\text{mol H}_2 \text{ min}^{-1} \text{ mg}^{-1}$ were achieved (Figure 1B). Our results suggest that the chemical self-assembly of the $[4\text{Fe}4\text{X}]_\text{H}$ cluster ($\text{X} = \text{S}, \text{Se}$) is a slow process compared to the

subsequent spontaneous activation of HYDA1 $[4\text{Fe}_\text{H}]$ by chemically synthesized $[2\text{Fe}_\text{H}]^{\text{MIM}}$.^[3a,b] However, differences in reaction kinetics are expected, as complete $[4\text{Fe}4\text{X}]_\text{H}$ assembly involves protein folding and passes through several metal cluster intermediates.^[8a] In contrast, incorporation of $[2\text{Fe}_\text{H}]^{\text{MIM}}$ only requires the formation of a single covalent bond and subsequent CO dissociation.^[3a,b] After 19 h of cluster reconstitution, H_2 -production activities of samples from $[2\text{Fe}_\text{H}]^{\text{MIM}}$ -activated crude mixtures for both cluster types reached 60% of the activity detected for the control sample of in vitro matured HYDA1 $[4\text{Fe}_\text{H}]$ expressed in *E. coli*. However, upon additional protein purification between reconstitution and in vitro maturation, which removes misfolded and aggregated HYDA1 $[\Delta\text{H}]$, specific activities of both enzyme variants (HYDA1 $[4\text{Fe}4\text{Se}]_\text{H}^{\text{MIM}}$ and HYDA1 $[4\text{Fe}4\text{S}]_\text{H}^{\text{MIM}}$) reached 85% of the wild-type activity (Figure 1C). Thus, replacing S^{2-} with Se^{2-} still allows for the subsequent incorporation of $[2\text{Fe}_\text{H}]^{\text{MIM}}$ and, moreover, does not alter the catalytic features of the H-cluster.

The kinetic parameters of the two chemically reconstituted HYDA1 $[4\text{Fe}4\text{X}]_\text{H}^{\text{MIM}}$ proteins were determined using both the artificial e^- -mediator methyl viologen (MV) and the native redox partner ferredoxin (PETF; Supporting Information, Figure S1 and Table S1). Both mediators are assumed to directly transfer electrons to the $[4\text{Fe}_\text{H}]$ cluster of HYDA1.^[13] The K_m and V_max values were similar to those from in vivo assembled HYDA1 $[4\text{Fe}_\text{H}]$ with synthetic $[2\text{Fe}_\text{H}]^{\text{MIM}}$ cluster^[3b] and correspond to previously published data for wild-type HYDA1.^[13b,14,15] To verify the successful chalcogenide exchange in reconstituted HYDA1 $[4\text{Fe}4\text{Se}]_\text{H}$, the protein was crystallized under anaerobic conditions and its structure determined using HYDA1 $[4\text{Fe}_\text{H}]$ (PDB ID 3LX4) as a reference model.^[16] The crystal structure allowed us to confirm the consistency of the overall protein structure with the native enzyme. Although the resolution of 3.1 \AA was not sufficient to determine deviations in cluster geometry, or the exact distances between Fe and chalcogenide atoms in reference

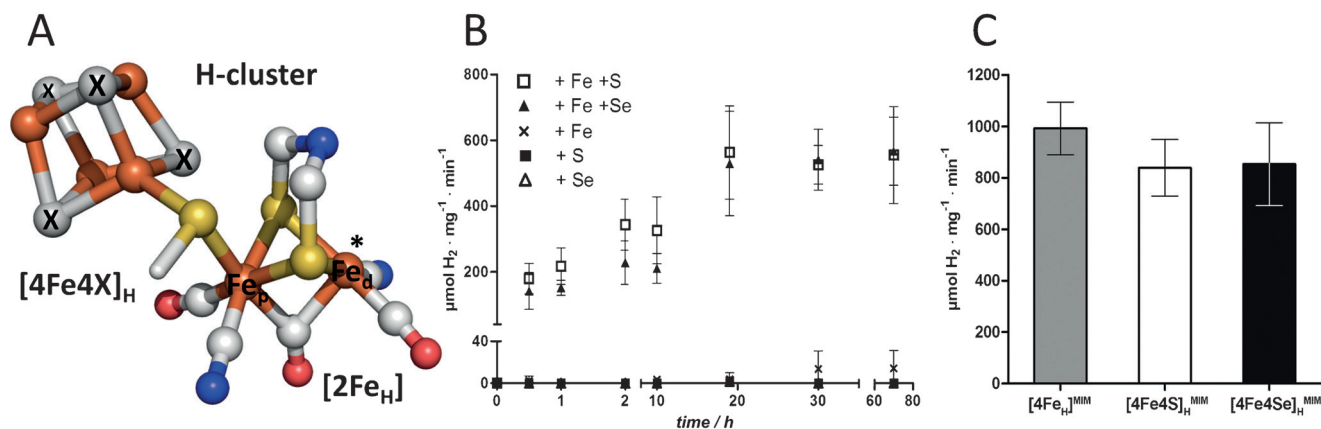


Figure 1. Cluster incorporation and specific H_2 -production rates of HYDA1 holoenzymes with S- and Se-reconstituted H-clusters. A) Ball and stick model of the chalcogenide-substituted cubane subcluster $[4\text{Fe}4\text{X}]_\text{H}$ as part of the H-cluster consisting of $[4\text{Fe}4\text{X}]_\text{H}$ ($\text{X} = \text{S}, \text{Se}$; gray) and $[2\text{Fe}_\text{H}]$ (PDB ID 3C8Y). * location of catalytic turnover. B) Time-dependency of the chemical HYDA1 $[4\text{Fe}4\text{X}]_\text{H}$ cubane cluster reconstitution by determination of the specific H_2 -production rates of the in vitro matured holoenzymes. Reconstitution reactions contained iron (Fe^{2+}) and either sulfide (S^{2-}) or selenide (Se^{2-}), while control mixtures only contained Fe^{2+} , S^{2-} , or Se^{2-} as indicated. C) For determining the specific H_2 -production activity, 10 nm of overnight (19 h)-reconstituted and purified HYDA1 $[4\text{Fe}4\text{X}]_\text{H}$ enzyme was measured compared to wild-type (HYDA1 $[4\text{Fe}_\text{H}]$) with a 10-fold excess of $[2\text{Fe}_\text{H}]^{\text{MIM}}$. All experiments were performed in triplicate and error bars represent the standard deviation.

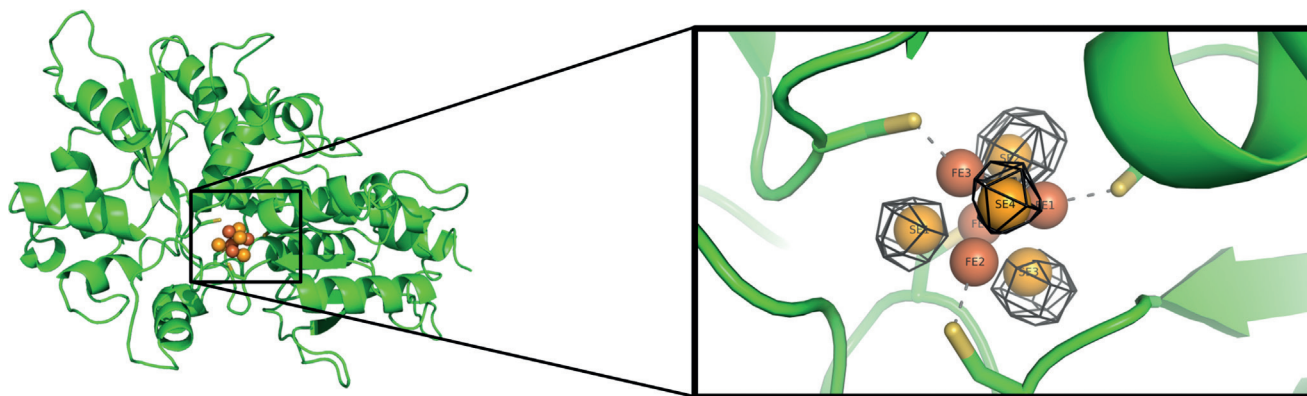


Figure 2. Crystal structure of HYDA1[4Fe4Se]_H and localization of Se atoms in the cubane cluster. Presented is a cartoon model of the HYDA1[4Fe4Se]_H structure at a resolution of 3.1 Å. A detailed view of the [4Fe4Se]_H cubane cluster is shown in the magnification with the Se anomalous electron density presented as a mesh. Selenide atoms were located at the sulfur positions of the reference cluster by calculating a difference map (black mesh; contoured at 6 σ) of the anomalous difference Fourier maps from datasets on and below the absorption edge of Se (protein backbone, green; Fe, brown; Se, ochre; cysteinyls, yellow).

to the standard [4Fe_H]-cluster, selenide atoms could be unambiguously located at the sulfide positions of the native reference cluster (PDB ID 3LX4) owing to the strong anomalous scattering of selenide at 12.666 keV (Figure 2 and Figure S2). To yield a selenium-specific anomalous difference Fourier map, single-crystal measurements of the anomalous signal on and below the Se K-edge were subtracted. The electron densities of this difference map did not significantly deviate from one cubane edge to another, indicating a homogeneous occupancy of Se atoms at all four cluster positions (Figure S3). Successful chalcogenide exchange was previously reported for the [4Fe4S]-cluster in dinitrogenase reductase (Fe-protein) of *Klebsiella pneumoniae*.^[12c] However, the resulting [4Fe4Se]-protein exhibited a five-fold decrease in ATP-specific e⁻-transfer rate compared to the native dinitrogenase, leading to an overall 20-fold reduction in specific activity. It was therefore possible that the chalcogenide exchange here could alter the redox properties of the [FeS]-clusters. This was found to be the case for ferredoxins,^[17] as well as for a model complex of the [2Fe_H] with selenium-substituted acid-labile sulfur atoms.^[18] The HYDA1 [4Fe_H]-cluster is a redox-active catalytic cofactor, thus any redox change to the cluster would also change the redox-dependent catalytic features of the enzyme. For example, for the radical SAM protein biotin synthase, the replacement of sulfur with selenide within the two iron–sulfur sites (the [4Fe4S]-cluster that coordinates and reduces S-adenosyl-methionine and the [2Fe2S]-cluster that donates sulfur for biotin formation) severely reduced the turnover of biotin synthesis by 70%.^[19] To determine whether the redox properties of the [2Fe_H]-subcluster were affected here, Fourier transform infrared (FTIR) spectroscopy was performed. FTIR spectroscopy can detect minor deviations in the structural arrangement as well as electron distribution of the [FeFe]-hydrogenase active site, which are reflected by shifts of absorbance bands in the vibrational spectrum of the Fe–C(=O/N) ligands in the [2Fe_H]-subcluster (Figure 1 A).^[1c,4,11,20] Accordingly, FTIR-measurements were conducted with both chalcogenide-reconstituted and in-vitro-matured HYDA1[4Fe4X]_H^{MIM}, and wild-type HYDA1-

[4Fe_H]_H^{MIM}. HYDA1 samples were converted to characteristic catalytic and non-catalytic states. To enable a spectral comparison of both reconstituted proteins to HYDA1[4Fe_H]_H^{MIM} in an unambiguously defined state, the three proteins were purged with 100% carbon monoxide gas (CO) prior to measurements leading to the homogeneous enrichment of the non-catalytic H_{ox}-CO state (Figure 3 a, b).^[4,11,20] Purging with N₂ led to a mixture of the three described catalytic resting states: H_{ox}, the oxidized ready state, and the two reduced states, H_{red} and H_{red}^[4,11] (Figure 3 c). A selective accumulation of H_{ox} was achieved by addition of thionine (Figure 3 d). Although all of the protein samples showed fractions of H_{ox}-CO, the specific CO and CN⁻ vibration signals for H_{ox} and both reduced states in HYDA1[4Fe4Se]_H^{MIM} fully matched the corresponding band positions of the respective control samples (Figure 3; Table S3).

The FTIR spectra thus confirmed both the stable incorporation of [2Fe_H]_H^{MIM} into reconstituted HYDA1[4Fe4X]_H proteins and an unaltered [2Fe_H]-ligand coordination/electron distribution of non-catalytic and catalytic states compared to wild-type HYDA1[4Fe_H]_H^{MIM} (Figure 3).^[3b,4] Upon comparison of the absorbance of the bridging CO (1820–1800 cm⁻¹) in H_{ox}-CO with the integral of the amide II band (1600–1485 cm⁻¹, omitted in Figure 3 for clarity), which was used as a measure of protein concentration, it was determined that [2Fe_H]_H^{MIM} had an occupancy of 61% in HYDA1-[4Fe4S]_H^{MIM} and 77% in HYDA1[4Fe4Se]_H^{MIM} compared to HYDA1[4Fe_H]_H^{MIM}. Di-iron-cluster occupancy and specific activities of the purified in vitro matured HYDA1-[4Fe4X]_H^{MIM} proteins were comparable and further corresponded to the features of the control sample, confirming that in vitro maturation of HYDA1[4Fe4Se]_H indeed results in a fully active variant of the unique and complex H-cluster. The results presented here, together with those from other recently published works,^[3b,21] demonstrate that both H-cluster parts can be derivatized without destroying catalytic activity. The fact that a [4Fe4Se]-cluster, as part of the H-cluster, displays full catalytic activity is of particular interest. It is well known from synthetic [4Fe4X(SR)₄]³⁻ (X = S, Se) cubanes that S and Se homologs show only small differences

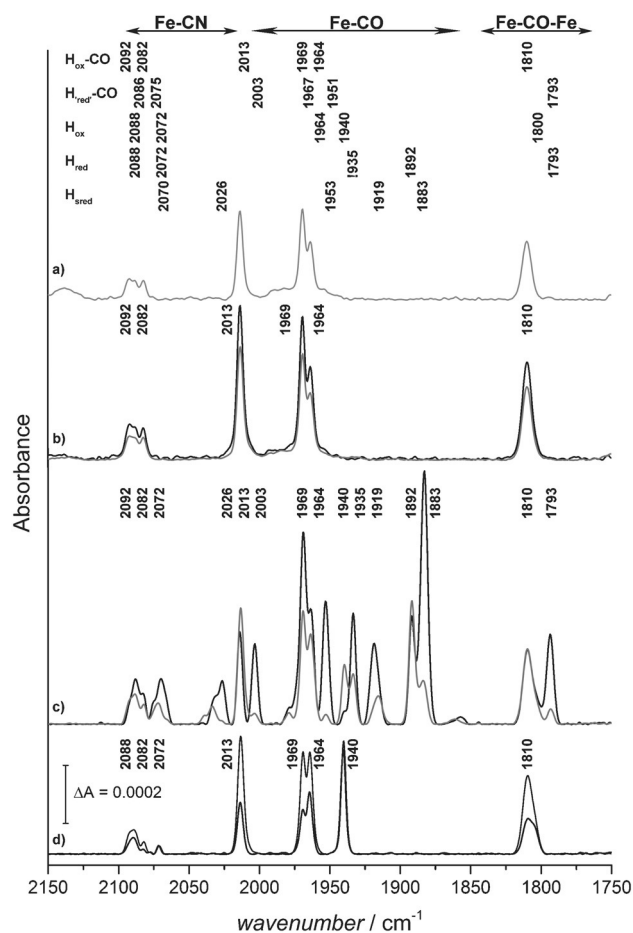


Figure 3. FTIR measurements of HYDA1[4Fe4X]_H^{MIM} in comparison to HYDA1[Fe_H]^{MIM}. Comparison of state-enriched CO/CN⁻-ligand spectra of the [2Fe_H]-subsite of wild-type protein and HYDA1 samples with reconstituted and matured H-cluster, normalized to the amide II signal of HYDA1[4Fe_H]^{MIM} and vertically displaced for clarity. a) HYDA1[4Fe4S]_H^{MIM} (150 μM) flushed with 100% CO prior to FTIR measurement to generate the defined H_{ox}-CO state of the [2Fe_H]-cofactor. b) HYDA1[4Fe4Se]_H^{MIM} (300 μM) red and HYDA1[4Fe_H]^{MIM} (150 μM) in black prepared as described for (a). c) HYDA1[4Fe4Se]_H^{MIM} (420 μM) and HYDA1[4Fe_H]^{MIM} (300 μM) after flushing with 100% N₂. d) HYDA1[4Fe4Se]_H^{MIM} (330 μM) and HYDA1[4Fe_H]^{MIM} (300 μM) oxidized with a 3-fold molar excess of thionine. State-annotation was adapted from Ref. [11].

in their basic structures, with the average Fe–Se bond being slightly larger (≈ 0.12 Å) compared to the Fe–S bond.^[22] Comparable force constants also reflect the similarity of the Fe–S and Fe–Se bonds.

Despite structural similarities, the electronic properties can differ significantly, as was shown by cyclic voltammetry on homologous [4Fe4X]-cluster compounds.^[22] Notably, [4Fe4Se]-complexes displayed more positive reduction potentials compared to their [4Fe4S] counterparts and were thus easier to reduce. This difference indeed should lead to an altered e⁻-exchange behavior between the [4Fe4Se]_H-cluster and the [2Fe_H]-subsite of the H-cluster variant presented here, which again should be reflected in shifted CO/CN⁻ ligand spectra for the different catalytic states of the latter subsite. This however is not deducible from any of the available

experimental data. Instead, the present study shows that selenium can act as a fully-fledged substitute for sulfur yielding a functional [FeFe]-hydrogenase. In addition, we herein provide evidence that the H-cluster tolerates electronic manipulations in the interplay of the [4Fe_H]-cluster and the [2Fe_H]-subsite. This seems unexpected given the fact that efficient subcluster communication is crucial for fulfilling the catalytic cycle. However, the FTIR-spectra of reduced HYDA1 matured in vitro with the non-natural derivative [Fe₂(CO)₄(CN)₂(pdt)]²⁻ of the [2Fe_H]-cofactor, which does not provide H₂ turnover activity, only showed minor shifts of 3–12 cm⁻¹ in the CO/CN⁻-band pattern compared to the oxidized state.^[11] This was attributed to the fact that, unlike the native [2Fe_H]-version, this single reduction step is restricted to the [4Fe_H]-site. Thus, while both subclusters are functionally coupled, the effect of changes in redox state and constitution of the [4Fe_H]-moiety on the catalytic features of the [2Fe_H]-site seem to be restricted. It can be assumed that chalcogenide substitution within the [2Fe_H]-site will more prominently affect the catalytic features and state-specific FTIR-band patterns as it directly modulates the electronic fine-structure of the actual location of catalytic turnover.

Having now the complementary tools of cubane cluster reconstitution and in vitro [2Fe_H]^{MIM} maturation of HYDA1, it is possible to individually label both clusters by site-directed exchange of a particular element within the H-cluster for advanced spectroscopic investigations. Moreover, the complete chemical incorporation allows for the inclusion of the whole H-cluster into next-generation enzyme engineering concepts.

The successful de novo synthesis of a functional H-cluster-type, as described here, will encourage other scientists to add another dimension, and thus level of quality, to their future enzyme design projects going beyond simple modulations in the protein environment.

Acknowledgements

We acknowledge the European Synchrotron Radiation Facility, Grenoble, France and the Paul Scherrer Institut, Villigen, Switzerland for provision of synchrotron radiation facilities, and we would like to thank the staff at beamlines ID29 (ESRF) and PXII (PSI-SLS) for assistance. We are grateful to Dr. Matthias Mueller and Dr. Mandy Miertzschke from the MPI of Molecular Physiology, Dortmund, Germany, for their help during data collection at the Paul Scherrer Institut. T.H. gratefully acknowledges support from the Deutsche Forschungsgemeinschaft (DFG) (DIP project cooperation “Nanoengineered optoelectronics with biomaterials and bioinspired assemblies”; Cluster of Excellence RESOLV, EXC1069), the Volkswagen Foundation (LigH2t), and the EU (Sun2Chem). U.-P.A. thanks the Fonds of the Chemical Industry (Liebig grant) and the Deutsche Forschungsgemeinschaft (Emmy Noether grant, AP242/2-1) for financial support.

Keywords: chalcogenide exchange · H₂ production · H-clusters · hydrogenases · selenium

How to cite: *Angew. Chem. Int. Ed.* **2016**, *55*, 8396–8400
Angew. Chem. **2016**, *128*, 8536–8540

- [1] a) C. Madden, M. D. Vaughn, I. Diez-Perez, K. A. Brown, P. W. King, D. Gust, A. L. Moore, T. A. Moore, *J. Am. Chem. Soc.* **2012**, *134*, 1577–1582; b) R. Cammack, *Nature* **1999**, *397*, 214–215; c) W. Lubitz, H. Ogata, O. Rüdiger, E. Reijerse, *Chem. Rev.* **2014**, *114*, 4081–4148; d) K. A. Vincent, A. Parkin, F. A. Armstrong, *Chem. Rev.* **2007**, *107*, 4366–4413.
- [2] a) J. Meyer, *Cell. Mol. Life Sci.* **2007**, *64*, 1063–1084; b) P. M. Vignais, B. Billoud, *Chem. Rev.* **2007**, *107*, 4206–4272; c) M. Winkler, J. Esselborn, T. Happe, *Biochim. Biophys. Acta Bioenerg.* **2013**, *1827*, 974–985.
- [3] a) G. Berggren, A. Adamska, C. Lambertz, T. R. Simmons, J. Esselborn, M. Atta, S. Gambarelli, J. M. Mouesca, E. Reijerse, W. Lubitz, T. Happe, V. Artero, M. Fontecave, *Nature* **2013**, *499*, 66–69; b) J. Esselborn, C. Lambertz, A. Adamska-Venkatesh, T. Simmons, G. Berggren, J. Noth, J. Siebel, A. Hemschemeier, V. Artero, E. Reijerse, M. Fontecave, W. Lubitz, T. Happe, *Nat. Chem. Biol.* **2013**, *9*, 607–609; c) D. W. Mulder, M. W. Ratzloff, M. Bruschi, C. Greco, E. Koonce, J. W. Peters, P. W. King, *J. Am. Chem. Soc.* **2014**, *136*, 15394–15402.
- [4] A. Adamska, A. Silakov, C. Lambertz, O. Rüdiger, T. Happe, E. Reijerse, W. Lubitz, *Angew. Chem. Int. Ed.* **2012**, *51*, 11458–11462; *Angew. Chem.* **2012**, *124*, 11624–11629.
- [5] a) J. Noth, R. Kositzki, K. Klein, M. Winkler, M. Haumann, T. Happe, *Sci. Rep.* **2015**, *5*, 13978; b) J. M. Kuchenreuther, C. S. Grady-Smith, A. S. Bingham, S. J. George, S. P. Cramer, J. R. Swartz, *PLoS ONE* **2010**, *5*, e15491.
- [6] a) R. Lill, U. Mühlenhoff, *Annu. Rev. Biochem.* **2008**, *77*, 669–700; b) R. Lill, *Nature* **2009**, *460*, 831–838; c) B. Roche, L. Aussel, B. Ezraty, P. Mandin, B. Py, F. Barras, *Biochim. Biophys. Acta Bioenerg.* **2013**, *1827*, 923–937.
- [7] a) J. B. Broderick, A. S. Byer, K. S. Duschene, B. R. Duffus, J. N. Betz, E. M. Shepard, J. W. Peters, *J. Biol. Inorg. Chem.* **2014**, *19*, 747–757; b) E. M. Shepard, F. Mus, J. N. Betz, A. S. Byer, B. R. Duffus, J. W. Peters, J. B. Broderick, *Biochemistry* **2014**, *53*, 4090–4104; c) J. M. Kuchenreuther, W. K. Myers, D. L. Suess, T. A. Stich, V. Pelmenschikov, S. A. Shiigi, S. P. Cramer, J. R. Swartz, R. D. Britt, S. J. George, *Science* **2014**, *343*, 424–427.
- [8] a) H. Beinert, R. H. Holm, E. Münck, *Science* **1997**, *277*, 653–659; b) R. Malkin, J. C. Rabinowitz, *Biochem. Biophys. Res. Commun.* **1966**, *23*, 822–827.
- [9] a) A. S. Pandey, T. V. Harris, L. J. Giles, J. W. Peters, R. K. Szilagyi, *J. Am. Chem. Soc.* **2008**, *130*, 4533–4540; b) J. W. Peters, W. N. Lanzilotta, B. J. Lemon, L. C. Seefeldt, *Science* **1998**, *282*, 1853–1858.
- [10] a) D. W. Mulder, D. O. Ortillo, D. J. Gardenghi, A. V. Naumov, S. S. Ruebush, R. K. Szilagyi, B. Huynh, J. B. Broderick, J. W. Peters, *Biochemistry* **2009**, *48*, 6240–6248; b) J. M. Kuchenreuther, J. A. Stapleton, J. R. Swartz, *PLoS One* **2009**, *4*, e7565.
- [11] A. Adamska-Venkatesh, D. Krawietz, J. Siebel, K. Weber, T. Happe, E. Reijerse, W. Lubitz, *J. Am. Chem. Soc.* **2014**, *136*, 11339–11346.
- [12] a) W. H. Orme-Johnson, R. E. Hansen, H. Beinert, J. C. Tsibris, R. C. Bartholomaeus, I. C. Gunsalus, *Proc. Natl. Acad. Sci. USA* **1968**, *60*, 368–372; b) J. Meyer, J. M. Moulis, J. Gaillard, M. Lutz, *Adv. Inorg. Chem.* **1992**, *38*, 73–115; c) P. C. Hallenbeck, G. N. George, R. C. Prince, R. N. Thorneley, *J. Biol. Inorg. Chem.* **2009**, *14*, 673–682.
- [13] a) M. Winkler, A. Hemschemeier, J. Jacobs, S. Stripp, T. Happe, *Eur. J. Cell Biol.* **2010**, *89*, 998–1004; b) K. Sybirna, P. Ezanno, C. Baffert, C. Leger, H. Bottin, *Int. J. Hydrogen Energy* **2013**, *38*, 2998–3002; c) S. Rumpel, J. F. Siebel, C. Fares, J. F. Duan, E. Reijerse, T. Happe, W. Lubitz, M. Winkler, *Energy Environ. Sci.* **2014**, *7*, 3296–3301.
- [14] a) G. von Abendorth, S. Stripp, A. Silakov, C. Croux, C. Soucaille, L. Girbal, T. Happe, *Int. J. Hydrogen Energy* **2008**, *33*, 6076–6081; b) I. Yacoby, L. T. Tegler, S. Pocheikailov, S. Zhang, P. W. King, *PLoS One* **2012**, *7*, e35886.
- [15] M. Winkler, S. Kuhlert, M. Hippler, T. Happe, *J. Biol. Chem.* **2009**, *284*, 36620–36627.
- [16] D. W. Mulder, E. S. Boyd, R. Sarma, R. K. Lange, J. A. Endrizzi, J. B. Broderick, J. W. Peters, *Nature* **2010**, *465*, 248–251.
- [17] J. M. Moulis, J. Meyer, *Biochemistry* **1982**, *21*, 4762–4771.
- [18] R. Trautwein, L. R. Almazahreh, H. Gork, W. Weigand, *Dalton Trans.* **2015**, *44*, 18780–18794.
- [19] B. Tse Sum Bui, T. A. Mattioli, D. Florentin, G. Bolbach, A. Marquet, *Biochemistry* **2006**, *45*, 3824–3834.
- [20] A. Silakov, C. Kamp, E. Reijerse, T. Happe, W. Lubitz, *Biochemistry* **2009**, *48*, 7780–7786.
- [21] J. F. Siebel, A. Adamska-Venkatesh, K. Weber, S. Rumpel, E. Reijerse, W. Lubitz, *Biochemistry* **2015**, *54*, 1474–1483.
- [22] M. A. Bobrik, E. J. Laskowski, R. W. Johnson, W. O. Gillum, J. M. Berg, K. O. Hodgson, R. H. Holm, *Inorg. Chem.* **1978**, *17*, 1402–1410.

Received: December 23, 2015

Revised: March 27, 2016

Published online: May 23, 2016